Morphological, immunohistochemical, and genomic analyses of papillary renal neoplasm with reverse polarity

清澤, 大裕

Human Pathology (2021) **112**, 48–58

ELSEVIER

Human PATHOLOGY

www.elsevier.com/locate/humpath

Original contribution

Morphological, immunohistochemical, and genomic analyses of papillary renal neoplasm with reverse polarity☆

Daisuke Kiyozawa MD [a], Kenichi Kohashi MD, PhD [a], Dai Takamatsu MD [a], Takeo Yamamoto MD [a], Masatoshi Eto MD, PhD [b], Takeshi Iwasaki MD [a,c], Junichi Motoshita MD, PhD [c], Tatsuro Shimokama MD, PhD [d], Mitsuru Kinjo MD, PhD [d], Yumi Oshiro MD, PhD [e], Hirotoshi Yonemasu MD, PhD [f], Yoshinao Oda MD, PhD [a,*]

[a] *Department of Anatomic Pathology, Graduate School of Medical Sciences, Kyushu University, Fukuoka, 812-8582, Japan*
[b] *Department of Urology, Graduate School of Medical Sciences, Kyushu University, Fukuoka, 812-8582, Japan*
[c] *Department of Pathology, JCHO Kyushu Hospital, Kitakyushu, 806-8501, Japan*
[d] *Department of Pathology, Steel Memorial Yawata Hospital, Kitakyushu, 805-8508, Japan*
[e] *Department of Pathology, Matsuyama Red Cross Hospital, Matsuyama, 790-8524, Japan*
[f] *Department of Pathology, Oita Red Cross Hospital, Oita, 870-0033, Japan*

Received 2 March 2021; revised 20 March 2021; accepted 24 March 2021

Available online 1 April 2021

Keywords:
Papillary renal neoplasm with reverse polarity;
Papillary renal cell carcinoma;
Next-generation sequencing;
KRAS

Summary Papillary renal neoplasm with reverse polarity (PRNRP) is a recently proposed entity of renal tumor. It shows a far better prognosis than papillary renal cell carcinoma (PRCC) and frequently has *KRAS* missense mutation. In this study, we compared 14 cases of PRNRP and 10 cases of PRCC type 1 (PRCC1) and type 2 (PRCC2) from clinical, morphological, immunohistochemical, and molecular biological perspectives. We subjected all PRNRP and PRCC cases to immunohistochemical analysis. Whole-exome sequencing using next-generation sequencing (NGS) was performed for six cases of PRNRP, three cases of PRCC1, and four cases of PRCC2. A search for *KRAS* gene mutation in the remaining eight cases of PRNRP was performed by polymerase chain reaction (PCR) sequencing. The results showed that all cases of PRNRP were pT1N0M0, none of which followed a course of recurrence or tumor-related death. Immunohistochemical analysis revealed diffuse staining of CK7, EMA, PAX8, and GATA3 but weak or negative staining of CD10, CD15, and AMACR in PRNRP. By NGS and PCR, *KRAS* missense mutation was detected in 11 of 14 PRNRP cases, although pathogenic *KRAS* mutation was not observed in PRCC1 and PRCC2. NGS analysis revealed less tumor mutation burden

☆ Competing interests: The authors declare that there are no conflicts of interest to disclose.

* Corresponding author. Department of Anatomic Pathology, Graduate School of Medical Sciences, Kyushu University, Maidashi 3-1-1, Higashi-ku, Fukuoka, 812-8582, Japan.
E-mail address: oda@surgpath.med.kyushu-u.ac.jp (Y. Oda).

https://doi.org/10.1016/j.humpath.2021.03.009

in PRNRP than in PRCC. PRNRP also showed no specific chromosomal copy number abnormalities, including gains of 7 and 17. In conclusion, we propose that PRNRP is a distinct condition from PRCC.

1. Introduction

Papillary renal cell carcinoma (PRCC) is the second most common phenotype of renal cell carcinoma (RCC) [1]. In 1997, Delahunt and Eble divided PRCC into two major categories, PRCC type 1 (PRCC1) and PRCC type 2 (PRCC2), for the first time [2]. This categorization has since been adapted. PRCC1 is characterized by low nuclear grade, scant basophilic or clear cytoplasm, and nonoverlapping nuclei [2,3]. In contrast, PRCC2 frequently shows pseudostratification of high-grade nucleus and has abundant eosinophilic cytoplasm [2,3]. These two tumors show different immunohistochemical profiles [4], and each has characteristic chromosomal aberrations, for instance, gains of chromosomes 7 and 17 in PRCC1 [5]. In 2016, The Cancer Genome Atlas (TCGA) research group revealed that PRCC1 was associated with *MET* mutation, whereas PRCC2 was a more heterogeneous group and had various genetic alterations such as *CDKN2A* silencing, *SETD2* mutations, *TFE3* fusions, increased expression of components of the NRF2−ARE2 pathway, and CpG island methylation [6]. This research indicated that these two tumors are genetically distinct from each other.

Occasionally, a certain type of renal tumor with features intermediate between those of PRCC1 and PRCC2 has been identified. These tumor cells have low-grade nucleus and abundant eosinophilic cytoplasm, and their nucleus is located at the apical surface of papillae without nuclear pseudostratification. This tumor was called "oncocytoid-type PRCC" or "oncocytic PRCC" in various studies [7−12]. In some reports, this tumor was described as having trisomy of chromosome 7 or 17 [10−12] or loss of the Y chromosome [12]. From these results, "oncocytic PRCC" was considered a variant of PRCC for nearly 20 years. This tumor is also mentioned in the WHO Bluebook as "oncocytic PRCC" [1]. In 2017, Saleeb et al. subclassified PRCC into four groups [13]. Among them, a subset of tumor named "PRCC, type 4/oncocytic low-grade variant" showed a morphological pattern similar to that of oncocytic PRCC and was characterized by specific GATA3 immunoreactivity [13].

In 2019, Al-Obaidy et al. used the term "papillary renal neoplasm with reverse polarity" (PRNRP) for the first time and proposed that it should be distinguished from PRCC1 and PRCC2 [14]. They characterized PRNRP as a tumor having thinly branching papillae or a rarely predominant tubular structure and oncocytic tumor cells with apically located low-International Society of Urological Pathology (ISUP)-grade nuclei, accompanying loose clusters of foamy macrophages and less frequent psammoma bodies [14]. In addition, in the same year, Al-Obaidy et al. reported that PRNRP frequently featured *KRAS* gene mutation [15]. Subsequently, the term "papillary renal neoplasm," not "papillary renal cell carcinoma," was applied by other study groups based on its extremely indolent behavior [16−19]. Genetic analysis of frequent *KRAS* gene mutation has also been reported by some investigators [16,17,19].

Despite the publication of these papers about PRNRP, many features of PRNRP remain unclear because of its rarity. In this study, we attempted to compare PRNRP and PRCC1/PRCC2 from clinical, morphological, immunohistochemical, and molecular biological perspectives by using whole-exome sequencing and to establish the concept of PRNRP.

2. Materials and methods

2.1. Patients and samples

From a total of 2820 formalin-fixed, paraffin-embedded (FFPE) specimens of surgically resected RCC from five facilities (Kyushu University Hospital, JCHO Kyushu Hospital, Steel Memorial Yawata Hospital, Matsuyama Red Cross Hospital, and Oita Red Cross Hospital), we reviewed 163 PRCC cases and detected 14 cases of PRNRP. The selected FFPE materials obtained from Kyushu University Hospital were registered between 1980 and 2019, and those obtained from other four facilities were registered between 2000 and 2019. PRNRP cases were detected according to the following criteria: predominant papillary architecture, abundant eosinophilic cytoplasm (nuclear/cytoplasmic ratio $\leq$0.5), ISUP/WHO nuclear grade 1 or 2, occasional nuclear clearing and inconspicuous nucleoli, and a single layer of nonoverlapping tumor cells located at the apical surface. On the other hand, we considered tumors predominantly composed of a tubular structure, tumors showing frequent multinucleation, and tumors with small, wrinkly, and hyperchromatic nuclei, as "mimics of PRNRP," with reference to a study by Al-Obaidy et al. [14], and excluded them. We also selected 10 typical cases of each of PRCC1 and PRCC2 as a control group. PRCC1 was defined by low nuclear grade (ISUP/WHO nuclear grade 1 or 2), scant basophilic cytoplasm, and nonoverlapping nuclei. PRCC2 was defined by pseudostratification of high-grade nucleus (ISUP/WHO nuclear grade 2 or 3) and abundant eosinophilic cytoplasm. The histological review was based on

Table 1 Detailed information on the primary antibodies.

Antibody	Source	Clone	Company	Dilution	Positive staining
CK7	Mouse monoclonal	OV-TL 12/30	Dako, Agilent Technologies, CA	1:50	Membrane
EMA	Mouse monoclonal	E29	Dako, Agilent Technologies, CA	Predilution	Membrane
PAX8	Mouse monoclonal	BC12	Biocare Medical, LLC	1:50	Nucleus
GATA3	Mouse monoclonal	L50-823	Sigma Aldrich	1:100	Nucleus
CD10	Mouse monoclonal	56C6	Leica Biosystems, Germany	Predilution	Membrane
CD15	Mouse monoclonal	MMA	Becton, Dickinson and Company	1:50	Membrane
AMACR	Rabbit monoclonal	13H4	Dako, Agilent Technologies, CA	1:1000	Cytoplasm

light microscopic examinations with hematoxylin−eosin (HE) staining, and three pathologists (D.K., D.T., and K.K.) independently evaluated the HE slides in a blinded fashion.

The patients' clinical features, including presence or absence of dialysis, age at surgery, sex, and pathologic TNM stage (eighth edition; T1a−T4, NX, N0 or N1, and M0 or M1), and histological features of PRNRP were examined.

2.2. Immunohistochemical analysis

We used 4-μm-thick FFPE tumor tissue sections for the immunohistochemical analysis of CK7, EMA, CD10, CD15, AMACR, PAX8, and GATA3. Except for CD15 staining, sections were pretreated with polyoxyethylene sorbitan monolaurate (CK7), sodium citrate (EMA, CD10), ethylenediaminetetraacetic acid (AMACR), or Target Retrieval Solution (PAX8 and GATA3). The primary monoclonal antibodies and these staining patterns are listed in Table 1. The results were defined based on the tumor proportion score (TPS), and we considered TPS >50% as positive.

2.3. Next-generation sequencing and data analysis

For genetic comparison between PRNRP and PRCC, whole-exome sequencing of tumor and normal kidney DNA was performed by next-generation sequencing (NGS). The selected cases were six PRNRP cases, three PRCC1 cases, and four PRCC2 cases, in all of which resection was performed after 2013. Genomic DNA from tumor and normal kidney was separately extracted from 10-μm-thick paraffin-embedded tissue using the solid-phase reversible immobilization method (FormaPure DNA Kit; Beckman Coulter), in accordance with the manufacturer's instructions. The quality and quantity of the DNA were evaluated using FastQC version 0.11.7 (Babraham Bioinformatics, UK) and trimmed using Trimmomatic version 0.38 by Cell Innovator Inc. The sequencing library was prepared by random DNA fragmentation and amplification using SureSelect XT (Agilent Technologies). The enriched DNA was sequenced on NovaSeq6000 (Illumina, Inc). We commissioned Macrogen Inc to perform library construction and DNA sequence. The sequence data were aligned to the hg19/GRCh37 human reference genome. Samtools 1.9 and bcftools 1.9 were used for variant calling and read mapping.

By removing mutation data obtained from paired normal renal tissue, we more accurately identified somatic single-nucleotide variants (SNVs) and small insertions and deletions (indels). Nonsynonymous SNVs including missense and nonsense (stop gain) mutations as well as SNVs that may affect gene splicing (splicing variant) were selected. These somatic alterations were annotated using the Ensembl Variant Effect Predictor (VEP) version 91.0 [20]. We picked up mutations classified as "pathogenic" and "likely pathogenic" by VEP, which were then manually curated using the Integrative Genomics Viewer.

Each case's tumor mutation burden (TMB) was calculated using VarScan version 2.3.8. Common and germline variants were filtered out with reference to the Catalogue of Somatic Mutations in Cancer database, common dbSNP database, ExAC database, and somatic-germline/zygosity algorithm. Subsequently, the subset of high-confidence variants having tumor variant allele fraction (VAF) >20%, normal VAF <5%, and a somatic P of <0.07 was determined. In addition, Gene Ontology (GO) analysis using Revigo (http://revigo.irb.hr/) and copy number alteration (CNA) analysis using CNVkit (https://cnvkit.readthedocs.io/en/stable/) were performed. TMB calculation, GO analysis, and CNA analysis were carried out by Cell Innovator Inc.

2.4. *KRAS* mutation analysis by polymerase chain reaction

KRAS mutation analysis by polymerase chain reaction (PCR) sequencing was performed on the remaining PRNRP cases that had not undergone NGS. For this, genomic DNA was extracted the same as for the NGS. The mutational hotspot of *KRAS* exon 2 was examined using the following primers: forward 5′-GGTACTGGTGGAGTATTTGATAG-3′ and reverse 5′-CTGTATCGTCAAGGCACTCTTG-3′. The PCR reaction was carried in a thermocycler (Tgradient; Biometra, Germany). Then, amplified PCR products were purified using FastGene Gel/PCR Extraction Kit (Nippon Genetics Co, Japan) and were also evaluated by direct sequencing using an ABI 3500xl genetic analyzer

(Applied Biosystems, Foster City, CA). The sequencing results were analyzed using FinchTV 1.4.0.

2.5. Statistical analysis

We used JMP Statistical Discovery Software (version 14.0; SAS, Cary, NC) for the statistical analyses. The comparisons between PRNRP and PRCC were performed by Wilcoxon test. Significance was defined at $P < 0.05$. We also used the Kaplan–Meier method to analyze the overall survival (OS) by comparing the Kaplan–Meier curves using the Wilcoxon test. OS was defined as the time from surgery to last follow-up or death because of the original renal tumor.

3. Results

3.1. Clinicopathological characteristics

The clinical characteristics of the 14 PRNRP cases (Cases 1–14) are listed in Table 2. In 3 of 14 cases, hemodialysis had been performed. The median age of the patients was 68.1 years (range: 47–82); six patients (42.9%) were male and eight (57.1%) were female. None of the cases was accompanied by clinical symptoms, and they had all been detected incidentally by radiological imaging. Tumor size ranged from 1.0 to 5.0 cm, and all tumors except one were categorized as pT1aN0M0 (only Case 8 was pT1bN0M0) according to the eighth edition TNM staging system. After surgery, no recurrence, metastasis, or tumor-related death occurred in the PRNRP cases during the follow-up period (Supplemental Fig. 1).

Morphological features of PRNRP are summarized in Table 2 and shown in Fig. 1A–F. As described previously, all cases showed predominant papillary architecture (Fig. 1A) and had abundant eosinophilic cytoplasm and round low-grade clear nucleus with inconspicuous nucleolus (Fig. 1B). Tumor cells were located at the apical surface of papillae, and there was no nuclear pseudostratification (Fig. 1B). In two cases (Cases 5 and 7), tumor cells focally possessed clear cytoplasm (Fig. 1C). Stromal edema in fibrovascular cores was occasionally seen in nine tumors (Fig. 1D). In three cases, there were a few foamy macrophages in the stroma (Fig. 1E). Ten tumors had a fibrous capsule (Fig. 1F) but showed no extracapsular extension. None of the 14 tumors contained psammoma body, microvascular invasion (micro-v), or tumor necrosis. These pathological features of PRNRP did not resemble typical PRCC1 (Fig. 1G) or PRCC2 (Fig. 1H).

3.2. Immunohistochemical results

The immunohistochemical results of PRNRP are summarized in Table 3 and Fig. 2A–D. All tumors exhibited diffuse and strong staining for CK7 (Fig. 2A), EMA, and

Table 2 Clinicopathological summary of papillary renal neoplasm with reverse polarity.

Case No.	Dialysis	Age	Sex	Symptoms	Size (cm)	pT	cN	M	Clear cell	Stromal edema	Foamy cell	Fibrous capsule	Psammoma body	Extracapsular extension	Micro-v	Necrosis
1	−	48	F	−	3	1a	0	0	−	+	−	+	−	−	−	−
2	+	58	F	−	1.3	1a	0	0	−	−	−	−	−	−	−	−
3	−	66	M	−	1.4	1a	0	0	−	+	−	+	−	−	−	−
4	+	65	F	−	1.2	1a	0	0	−	−	−	−	−	−	−	−
5	−	47	M	−	1.2	1a	0	0	+	+	+	+	−	−	−	−
6	−	82	F	−	1	1a	0	0	−	+	−	+	−	−	−	−
7	+	77	F	−	3	1a	0	0	+	+	−	+	−	−	−	−
8	−	78	M	−	5	1b	0	0	−	+	+	−	−	−	−	−
9	−	72	M	−	1.4	1a	0	0	−	+	−	+	−	−	−	−
10	−	68	F	−	2	1a	0	0	−	+	−	+	−	−	−	−
11	−	66	M	−	1.7	1a	0	0	−	−	+	+	−	−	−	−
12	−	79	F	−	1	1a	0	0	−	−	−	+	−	−	−	−
13	−	73	M	−	1.7	1a	0	0	−	−	−	−	−	−	−	−
14	−	75	F	−	3	1a	0	0	−	+	−	+	−	−	−	−

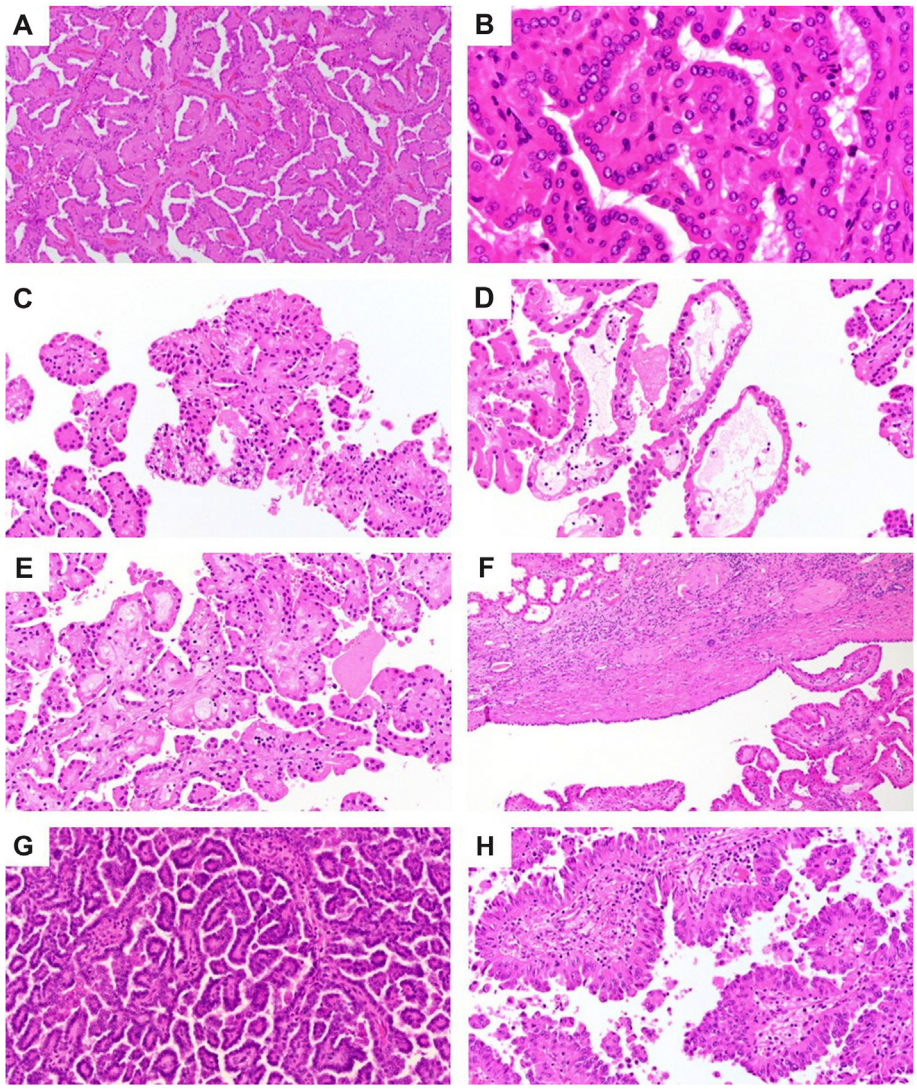

Fig. 1 Histological features of PRNRP and PRCC. PRNRP shows predominant papillary architecture (A) and has abundant eosinophilic cytoplasm and round low-grade clear nucleus with inconspicuous nucleolus, being located at the apical surface of papillae without nuclear pseudostratification (B). PRNRP focally contains clear cytoplasm (C). Stromal edema in fibrovascular cores is occasionally seen (D). A few foamy macrophages are observed in the stroma (E). PRNRP has a fibrous capsule but shows no extracapsular extension (F). PRCC1 is characterized by low nuclear grade, scant basophilic cytoplasm, and nonoverlapping nuclei (G). PRCC2 is characterized by pseudostratification of high-grade nucleus and abundant eosinophilic cytoplasm (H).

PAX8. GATA3 showed diffuse and moderate to strong staining (Fig. 2B). In contrast, 13 of the 14 cases were completely CD10 negative, with the 14th case showing focal CD10 staining (Case 6; Fig. 2C). CD15 was consistently negative. Eight of the 14 cases showed diffuse AMACR staining, although the intensity of tumor cells was weaker than that of renal tubule in nontumor areas (Fig. 2D).

Comparisons between PRNRP and PRCC1/PRCC2 are summarized in Table 4. There were significant differences between PRNRP and PRCC2 for CK7, EMA, and CD15. In addition, significant differences between PRNRP and PRCC1 and between PRNRP and PRCC2 were observed for GATA3, CD10, and AMACR.

3.3. Comparative genetic analysis between PRNRP and PRCC

Pathogenic gene mutations detected by whole-exome sequencing are shown in Fig. 3. NGS revealed *KRAS* missense mutation in four of six PRNRP cases. The detailed *KRAS* mutation types are listed below. Other mutations found in PRNRP included *BRIP1* nonsense mutation (c.2392C > T, p.Arg798Ter), *RAD50* nonsense mutation (c.3229C > T, p.Arg1077Ter), and *BRCA2* nonsense mutation (c.2677C > T, p.Gln893Ter). In PRCC1, *MET* missense mutation (c.3334C > T, p.His1112Tyr) was observed in one case. In PRCC2, one case had *NF2* nonsense mutation (c.169C > T, p.Arg57Ter), and two

Table 3 Results of immunohistochemistry and *KRAS* mutation analysis in papillary renal neoplasm with reverse polarity.

Case No.	CK7	EMA	PAX8	GATA3	CD10	CD15	AMACR
1	+	+	+	+	−	−	+
2	+	+	+	+	−	−	+
3	+	+	+	+	−	−	+
4	+	+	+	+	−	−	+
5	+	+	+	+	−	−	−
6	+	+	+	+	−	−	−
7	+	+	+	+	−	−	−
8	+	+	+	+	−	−	+
9	+	+	+	+	−	−	−
10	+	+	+	+	−	−	−
11	+	+	+	+	−	−	+
12	+	+	+	+	−	−	+
13	+	+	+	+	−	−	+
14	+	+	+	+	−	−	−

KRAS mutation (by NGS)	KRAS mutation (by PCR)
	G12D(Codon12 GGT(Gly)→GAT(Asp))
	–
	G12C(Codon12 GGT(Gly)→TGT(Cys))
	G12V(Codon12 GGT(Gly)→GTT(Val))
	G12D(Codon12 GGT(Gly)→GAT(Asp))
	G12V(Codon12 GGT(Gly)→GTT(Val))
	G12V(Codon12 GGT(Gly)→GTT(Val))
	G12V(Codon12 GGT(Gly)→GTT(Val))
–	
G12V(Codon12 GGT(Gly)→GTT(Val))	
G12V(Codon12 GGT(Gly)→GTT(Val))	
G12R(Codon12 GGT(Gly)→CGT(Arg))	
–	
G12V(Codon12 GGT(Gly)→GTT(Val))	

cases showed *SETD2* nonsense mutation (one had c.4792C > T, p.Arg1598Ter, and the other had c.4774C > T, p.Arg1592Ter). Moreover, there were no gene alterations common to PRNRP and PRCC1/PRCC2.

Significant GO terms in each tumor type are described in Supplemental Fig. 2. Enriched terms in PRNRP were associated with O-glycan processing, detection of chemical stimulus, protein localization, calcium-dependent cell−cell adhesion, and single fertilization. The first two groups were also observed in PRCC1 and PRCC2, but individual enriched terms in each tumor were different.

3.4. TMB analysis between PRNRP and PRCC

The TMB of each tumor was calculated. In PRNRP, it ranged from 1.7 to 30.7 (mean: 6.9) mutations per megabase

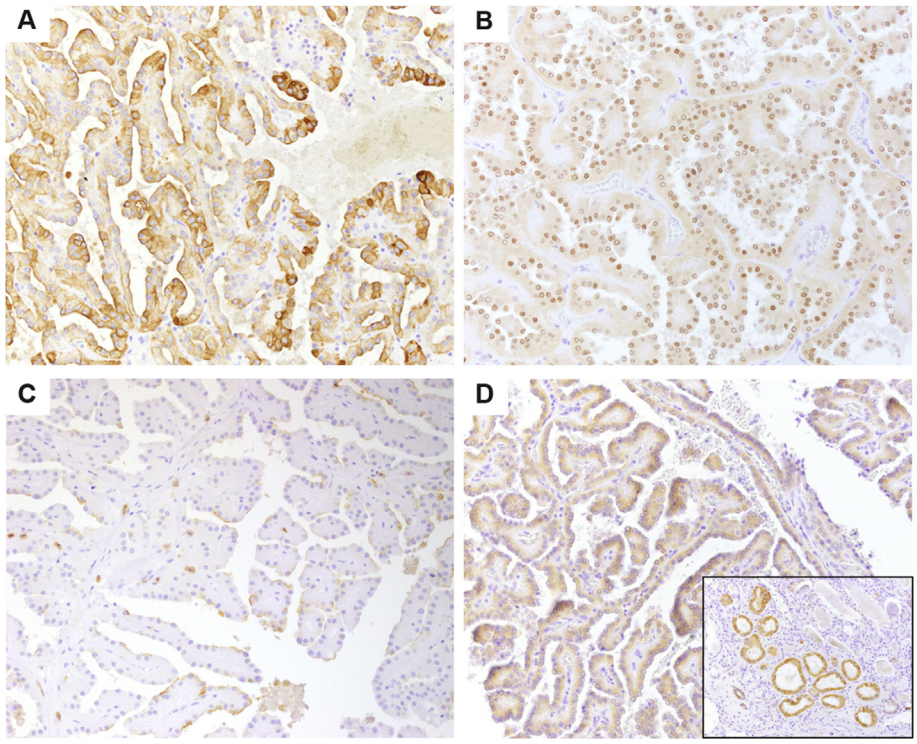

Fig. 2 Immunohistochemical profile of PRNRP. Tumor cells are diffusely positive for CK7 (A) and GATA3 (B) but negative or focally positive for CD10 (C). AMACR shows a weak reaction (D) compared with normal renal tubules (D, inset).

Table 4 Comparison of immunohistochemical profile between papillary renal neoplasm with reverse polarity (PRNRP) and papillary renal cell carcinoma (PRCC).

Antibody	PRNRP (n = 14)	PRCC1 (n = 10)	PRCC2 (n = 10)	*P* PRNRP *vs.* PRCC1	*P* PRNRP *vs.* PRCC2
CK7	14	9	4	0.4167	0.0016
EMA	14	9	5	0.4167	0.0059
PAX8	14	8	7	0.163	0.0593
GATA3	14	0	0	<0.0001	<0.0001
CD10	0	8	8	<0.0001	<0.0001
CD15	0	3	5	0.0593	0.0059
AMACR	8	10	10	0.0239	0.0239

pair (/MB). In five of the six cases, TMB was less than 3.3 mutations/MB (range 1.7−3.3), whereas the sixth case, which lacked KRAS mutation (Case 13), had 30.7 mutations/MB. The TMB of PRNRP was significantly lower than those of PRCC1 (26.5−204.2, mean: 101.7 mutations/MB) and PRCC2 (6.2−150.3, mean: 64.2/MB; Fig. 4).

3.5. Genome-wide CNAs detected in PRNRP, PRCC1, and PRCC2 groups

The chromosomal CNAs in each tumor groups (PRNRP, PRCC1, and PRCC2) are described in Fig. 5. The six samples of PRNRP cases showed a consistent pattern compared with PRCC1 and PRCC2. One case had chromosome 14 loss only, but other PRNRP cases showed no obvious chromosomal abnormalities, including gains of 7 and 17. In PRCC1 and PRCC2, gains of chromosome 7 and 17 and loss of chromosome 14 were more frequently observed. Losses of chromosome 4, 5q, 9, 13, and 15 were focally detected in PRCC2 cases.

3.6. Evaluation of KRAS gene mutation in PRNRP

KRAS gene mutations detected by NGS are described in Fig. 6. Three of these four involved c.35G > T (p.Gly12Val and G12V), and the other was c.34G > C (p.Gly12Arg and G12R). *KRAS* gene mutation was also detected in seven of the eight PRNRP cases analyzed by PCR sequencing. These *KRAS* mutation types were G12V (four cases), G12D (two cases), and G12C (one case; Fig. 7). In total, 11 of the 14 cases (78.6%) contained *KRAS* exon 2 missense mutation (Table 3).

4. Discussion

Before Al-Obaidy et al. used the term “papillary renal neoplasm with reverse polarity” for the first time, various articles discussing so-called “oncocytic PRCC” had been published [7−12]. In these articles, “oncocytic PRCC” was reported to show wide morphological, immunohistochemical, and prognostic variation. For instance, many

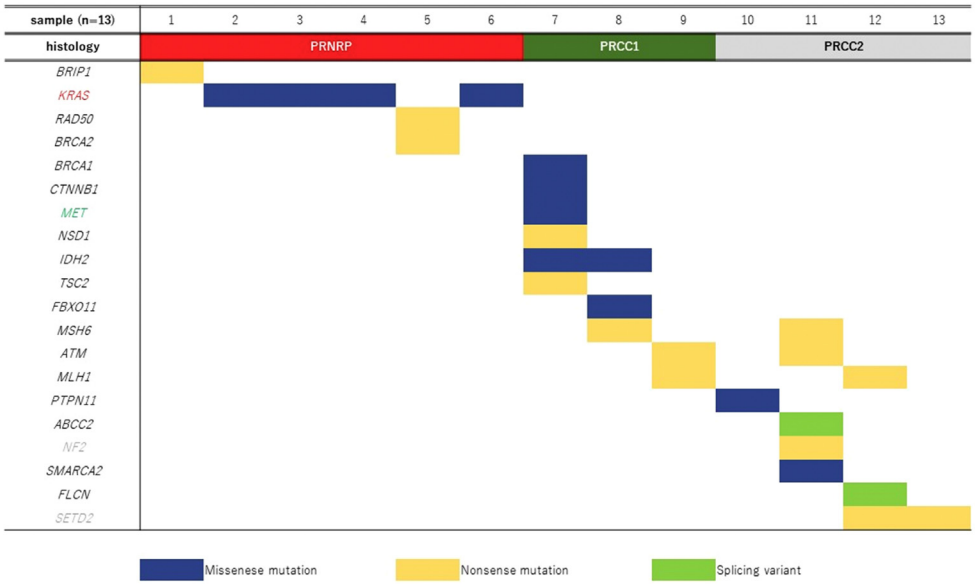

Fig. 3 Next-generation sequencing results on six PRNRP, three PRCC1, and four PRCC2 cases. *KRAS* missense mutation was detected in four of the six PRNRP cases, whereas there were no *KRAS* mutations in PRCC1 and PRCC2.

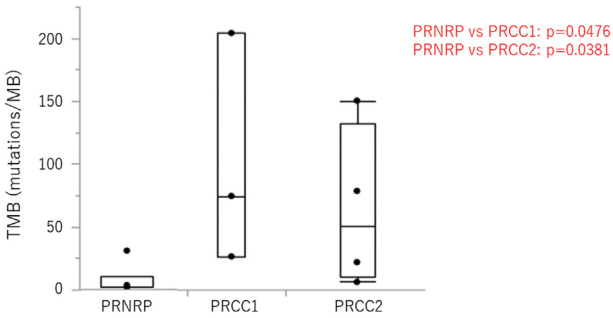

Fig. 4 TMB comparison between PRNRP and PRCC. The TMB of PRNRP was significantly lower than those of PRCC1 and PRCC2.

cases of "oncocytic PRCC" had a favorable prognosis, whereas a few aggressive cases such as those accompanied by sarcomatoid change and brain or bone metastasis were also reported [9,12]. However, we reviewed these articles keeping the morphological features of both PRNRP and its mimics in mind and noticed several tumors illustrated in these papers that seemed to resemble not pure PRNRP, but rather its mimics. In our study, we successfully excluded these mimics and could identify pure cases of PRNRP.

We found 14 cases of PRNRP among 163 resected renal papillary tumors (8.6%). In the recent literature, approximately 80 cases of PRNRP have been reported [14−19], which indicates the rarity of PRNRP. All cases had a low TNM stage and were shown to have a favorable prognosis in follow-up, without any recurrence, metastasis, or tumor-related death. Histologically, PRNRP showed a uniform morphological pattern, and cytological or structural polymorphisms were inconspicuous. PRNRP was rarely associated with tight clusters of foamy macrophages and psammoma bodies, which are typically observed in PRCC1 and PRCC2. Many of the PRNRP cases had a fibrous capsule, and there were no histological findings suggesting high-grade malignancy, such as extracapsular extension, microscopic vascular invasion, or tumor necrosis. Although the presence of eosinophilic cytoplasm was histologically similar to PRCC2, PRNRP was considered as low-grade tumor based on nuclear feature and provided clinical follow-up data. From these results and past literature [14−19], we support naming this tumor not "papillary renal cell carcinoma" but "papillary renal neoplasm." However, because of limited follow-up period, a possibility that this tumor is low-grade carcinoma cannot be completely denied.

In the immunohistochemical analysis, all PRNRP cases showed diffuse expression of CK7, EMA, and GATA3, whereas their expression of CD10, CD15, and AMACR occurred less frequently or was weaker than that of PRCC1 and PRCC2. In previous reports, it was revealed that PRNRP showed diffuse LCAM expression in addition to CK7, EMA, and GATA3 [14,17]. Tong et al. found staining for CK7, EMA, GATA3, and L1CAM in the renal distal tubules and proposed that PRNRP may potentially originate from the distal tubule [17]. Negative or focal expression of CD10, CD15, and AMACR, which are known as renal proximal tubule markers [21,22], also supports this hypothesis.

NGS and PCR sequencing revealed that PRNRP had *KRAS* missense mutation at a high frequency (11/14, 78.6%). There were G12V (7/11, 63.6%), G12D (2/11, 18.1%), G12C (1/11, 9%), and G12R (1/11, 9%). In previous studies, these four *KRAS* mutations at hotspot codon 12 were observed in PRNRP cases at rates from 80% to 90% [15−17,19]. In contrast, *KRAS* mutation is rarely detected in RCC. Only

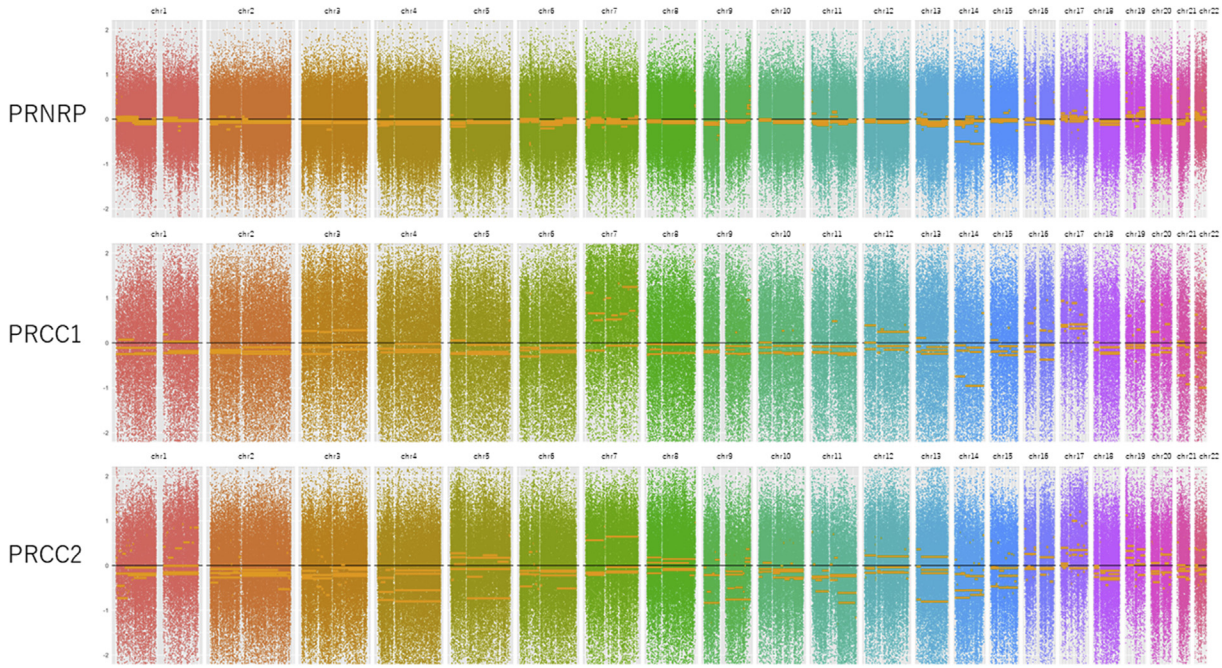

Fig. 5 Genome-wide view of copy number alterations. All chromosomes are color coded, and tracks consist of dots, which are calculated copy number. PRNRP showed a consistent pattern compared with PRCC1 and PRCC2 and lacked specific chromosomal abnormalities including gains of chromosome 7 and 17.

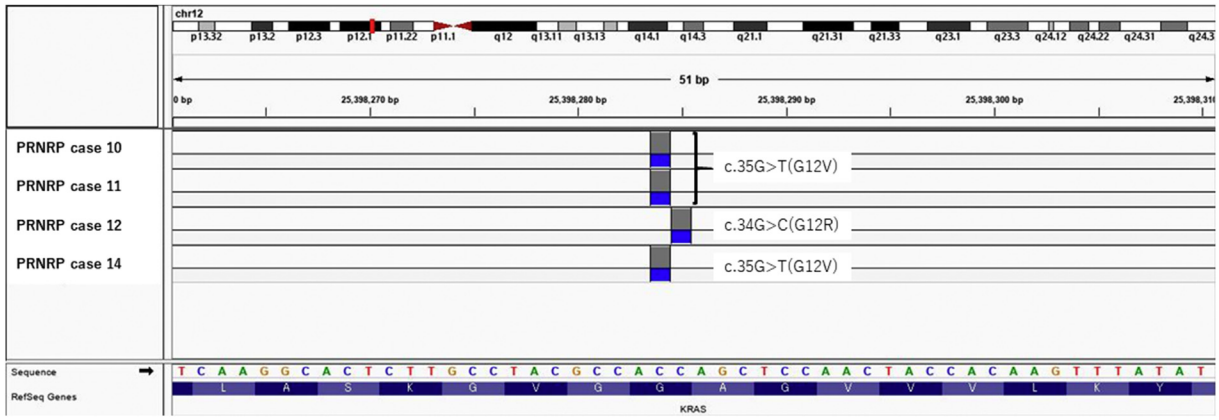

Fig. 6 Integrative Genomics Viewer snapshot of *KRAS* missense mutations identified in four PRNRP cases. Three cases showed p.Gly12Val (G12V) and one showed p.Gly12Arg (G12R).

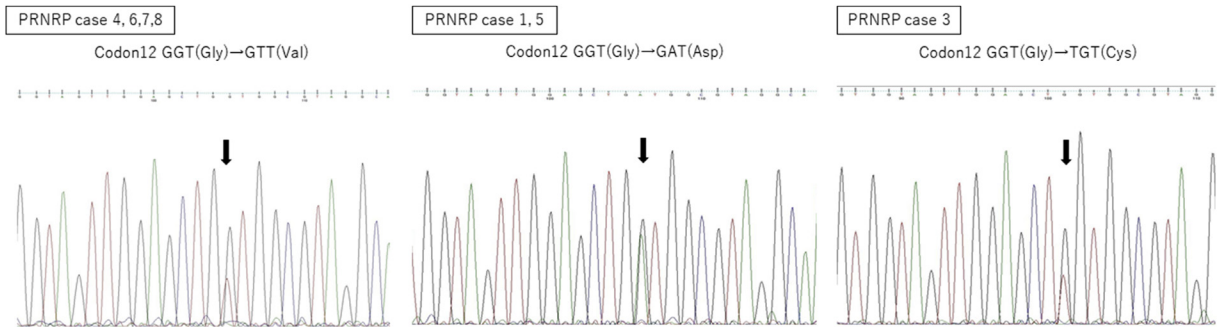

Fig. 7 PCR sequencing of *KRAS* hotpot mutations in PRNRP. There were G12V (four cases), G12D (two cases), and G12C (one case).

Raspollini et al. documented a case of RCC having *KRAS* mutation [23]. Some previous studies reported that clear cell RCC, PRCC, and chromophobe RCC lacked *KRAS* mutation [24−26]. In TCGA data set, five tumors having *KRAS* mutation are registered as PRCC [15]. Al-Obaidy et al., Kim et al., and Tong et al. reviewed these tumors independently and concluded that two or three tumors among them quite strongly resembled PRNRP [15−17].

The TMB of PRNRP was significantly lower than those of PRCC1 and PRCC2. TMB was less than 3.3/MB in five of the six PRNRP cases, but 30.7/MB in the sixth case lacking *KRAS* mutation. In the previously mentioned TCGA analysis, TMB in the three tumors suspected of being PRNRP and having *KRAS* mutation was also low ($\leq$20 mutations) [15,17]. These results suggest that *KRAS* mutation is one of the major genes responsible for PRNRP.

Other somatic mutations observed in PRNRP were in *BRIP1*, *RAD50*, and *BRCA2*. All of them were found in cases without *KRAS* mutation. These genes play important roles in DNA repair, and germline mutations in them are related to familial ovarian cancer and breast cancer [27,28]. Al-Obaidy et al. also found *BRCA2* mutation and gene duplication in two PRNRP cases [15]. However, considering the low TMB of PRNRP, it is doubtful whether mutations of these DNA repair genes induce tumor development. Mutations observed in PRCC1 or PRCC2, including in *MET*, *NF2*, and *SETD2*, could not be detected in PRNRP. GO enrichment analysis also revealed genetic differences between PRNRP and PRCC1/2.

PRNRP also exhibited a consistently distinct chromosomal pattern from PRCC1 and PRCC2, and this also supports the genetic difference between PRNRP and PRCC. Gains of chromosomes 7 and 17 had been thought to be associated with PRNRP [14], but we could not detect these specific chromosomal abnormalities in this study. In the past research, chromosome 7 and 17 trisomy in PRNRP were observed by fluorescence in situ hybridization (FISH) [14]. On the other hand, these chromosomal gains are detected in a nonneoplastic tubular epithelium in end-stage kidney disease [29], and the past FISH analysis may not reflect the true CNAs in the tumor cells. Deletion of chromosome 14, observed in one PRNRP case and some PRCC cases, can be found in other renal tumors, such as clear cell RCC, collecting duct carcinoma or renal oncocytoma [30]. In clear cell RCC, loss of chromosome 14q associates with poor clinical outcomes via a decrease in hypoxia inducible factor 1α messenger RNA and protein [31]; however, prognostic effects of chromosome 14 loss in other renal neoplasms have been still unknown.

The biological behavior of PRNRP may be also different from that of renal papillary adenoma. Morphologically, papillary adenoma has tumor cells with scant basophilic cytoplasm and low-grade nucleus [32] and strongly express AMACR by IHC [32], and these features resemble PRCC1 rather than PRNRP. Chromosomal aberrations of papillary adenoma are characterized by trisomy of chromosomes 7 and 17 and loss of the Y chromosome [32,33], which are observed in PRCC1 [5]. Based on these facts, papillary adenoma is considered to be a precursor lesion of PRCC. In contrast, GATA3 expression or *KRAS* gene mutation in papillary adenoma has yet to be comprehensively studied, and the relationship between PRNRP and papillary adenoma should be analyzed in future work.

In conclusion, PRNRP was characterized by uniform morphological pattern. On immunohistochemical analysis, PRNRP showed diffuse expression of distal tubule markers rather than proximal tubule markers. Frequent *KRAS* mutation, low TMB, and lacking specific chromosome abnormalities distinguished PRNRP from PRCC. From these results, PRNRP should be classified as a distinct subset of renal neoplasm and is considered to be distinct from especially high-grade PRCC2. PRNRP may become a distinct entity with benign behavior if further evidence are detected in the future.

Ethical approval

The institutional review board at Kyushu University approved this study (approval code: 2019-434).

Appendix A. Supplementary data

Supplementary data to this article can be found online at https://doi.org/10.1016/j.humpath.2021.03.009.

References

[1] Moch H, Humphrey PA, Ulbright TM, Reuter VE, editors. World Health Organization classification of tumours of the urinary system and male genital organs. 4th ed. Lyon: IARC Press; 2016.
[2] Delahunt B, Eble JN. Papillary renal cell carcinoma: a clinicopathologic and immunohistochemical study of 105 tumors. Mod Pathol 1997;10:537−44.
[3] Delahunt B, Eble JN, McCredie MR, Bethwaite PB, Stewart JH, Bilous AM. Morphologic typing of papillary renal cell carcinoma: comparison of growth kinetics and patient survival in 66 cases. Hum Pathol 2001;32:590−5.
[4] Alomari AK, Nettey OS, Singh D, Kluger H, Adeniran AJ. Clinicopathological and immunohistochemical characteristics of papillary renal cell carcinoma with emphasis on subtyping. Hum Pathol 2015;46:1418−26.
[5] Chevarie-Davis M, Riazalhosseini Y, Arseneault M, Aprikian A, Kassouf W, Tanguay S, et al. The morphologic and immunohistochemical spectrum of papillary renal cell carcinoma: study including 132 cases with pure Type 1 and Type 2 morphology as well as tumors with overlapping features. Am J Surg Pathol 2014;38:887−94.
[6] Cancer Genome Atlas Research Network, Linehan WM, Spellman PT, et al. Comprehensive molecular characterization of papillary renal-cell carcinoma. N Engl J Med 2016;374:135−45.
[7] Allory Y, Ouazana D, Boucher E, Thiounn N, Vieillefond A. Papillary renal cell carcinoma. Prognostic value of morphological subtypes in a clinicopathologic study of 43 cases. Virchows Arch 2003;442:336−42.
[8] Lefèvre M, Couturier J, Sibony M, Bazille C, Boyer K, Callardet P, et al. Adult papillary renal tumor with oncocytic cells: clinicopathologic, immunohistochemical, and cytogenetic features of 10 cases. Am J Surg Pathol 2005;29:1576−81.

[9] Hes O, Brunelli M, Michal M, Rocca PC, Hora M, Chilosi M, et al. Oncocytic papillary renal cell carcinoma: a clinicopathologic, immunohistochemical, ultrastructural, and interphase cytogenetic study of 12 cases. Ann Diagn Pathol 2006;10:133–9.
[10] Kunju LP, Wojno K, Wolf Jr JS, Cheng L, Shah RB. Papillary renal cell carcinoma with oncocytic cells and nonoverlapping low grade nuclei: expanding the morphologic spectrum with emphasis on clinicopathologic, immunohistochemical and molecular features. Hum Pathol 2008;39:96–101.
[11] Xia QY, Rao Q, Shen Q, Shi SS, Li L, Liu B, et al. Oncocytic papillary renal cell carcinoma: a clinicopathological study emphasizing distinct morphology, extended immunohistochemical profile and cytogenetic features. Int J Clin Exp Pathol 2013;6:1392–9.
[12] Han G, Yu W, Chu J, Liu Y, Jiang Y, Li Y, et al. Oncocytic papillary renal cell carcinoma: a clinicopathological and genetic analysis and indolent clinical course in 14 cases. Pathol Res Pract 2017;213:1–6.
[13] Saleeb RM, Brimo F, Farag M, Brodeur AR, Rotondo F, Beharry V, et al. Toward biological subtyping of papillary renal cell carcinoma with clinical implications through histologic, immunohistochemical, and molecular analysis. Am J Surg Pathol 2017;41:1618–29.
[14] Al-Obaidy KI, Eble JN, Cheng L, Williamson SR, Sakr WA, Gupta N, et al. Papillary renal neoplasm with reverse polarity: a morphologic, immunohistochemical, and molecular study. Am J Surg Pathol 2019;43:1099–111.
[15] Al-Obaidy KI, Eble JN, Nassiri M, Cheng L, Eldomery MK, Williamson SR, et al. Recurrent KRAS mutations in papillary renal neoplasm with reverse polarity. Mod Pathol 2020;33:1157–64.
[16] Kim SS, Cho YM, Kim GH, Kee KH, Kim HS, Kim KM, et al. Recurrent KRAS mutations identified in papillary renal neoplasm with reverse polarity—a comparative study with papillary renal cell carcinoma. Mod Pathol 2020;33:690–9.
[17] Tong K, Zhu W, Fu H, Cao F, Wang S, Zhou W, et al. Frequent KRAS mutations in oncocytic papillary renal neoplasm with inverted nuclei. Histopathology 2020;76:1071–83.
[18] Zhou L, Xu J, Wang S, Yang X, Li C, Zhou J, et al. Papillary renal neoplasm with reverse polarity: a clinicopathologic study of 7 cases. Int J Surg Pathol 2020;28:728–34.
[19] Chang HY, Hang JF, Wu CY, Lin TP, Chung HJ, Chang YH, et al. Clinicopathological and molecular characterization of papillary renal neoplasm with reverse polarity and its renal papillary adenoma analogue. Histopathology 2020 [Online ahead of print].
[20] McLaren W, Gil L, Hunt SE, Riat HS, Ritchie GRS, Thormann A, et al. The ensembl variant effect predictor. Genome Biol 2016;17:122.
[21] Shen SS, Ro JY, Tamboli P, Truong LD, Zhai Q, Jung SJ, et al. Mucinous tubular and spindle cell carcinoma of kidney is probably a variant of papillary renal cell carcinoma with spindle cell features. Ann Diagn Pathol 2007;11:13–21.
[22] Truong LD, Shen SS. Immunohistochemical diagnosis of renal neoplasms. Arch Pathol Lab Med 2011;135:92–109.
[23] Raspollini MR, Castiglione F, Martignoni G, Lapini A, Cheng L, Montironi R, et al. Multiple and bilateral kidney tumors with clear cells of three different histotypes: a case report with clinicopathologic and molecular study. APMIS 2016;124:619–23.
[24] Gattenlohner S, Etschmann B, Riedmiller H, Muller-Hermelink HK. Lack of KRAS and BRAF mutation in renal cell carcinoma. Eur Urol 2009;55:1490–1.
[25] Szymanska K, Moore LE, Rothman N, Chow WH, Waldman F, Jaeger E, et al. TP53, EGFR, and KRAS mutations in relation to VHL inactivation and lifestyle risk factors in renal-cell carcinoma from central and eastern Europe. Canc Lett 2010;293:92–8.
[26] Bayrak O, Sen H, Bulut E, Cengiz B, Karakok M, Erturhan S, et al. Evaluation of EGFR, KRAS and BRAF gene mutations in renal cell carcinoma. J Kidney Cancer VHL 2014;1:40–5.
[27] Suszynska M, Ratajska M, Kozlowski P. BRIP1, RAD51C, and RAD51D mutations are associated with high susceptibility to ovarian cancer: mutation prevalence and precise risk estimates based on a pooled analysis of ~30,000 cases. J Ovarian Res 2020;13:50.
[28] Ho V, Chung L, Singh A, Lea V, Revoltar M, Lim AH, et al. Early postoperative low expression of RAD50 in rectal cancer patients associates with disease-free survival. Cancers 2017;9:163.
[29] Hes O, Síma R, Nemcová J, Hora M, Bulimbasic S, Kazakov DV, et al. End-stage kidney disease: gains of chromosomes 7 and 17 and loss of Y chromosome in non-neoplastic tissue. Virchows Arch 2008;453:313–9.
[30] Yap NY, Rajandram R, Ng KL, Pailoor J, Fadzli A, Gobe GC. Genetic and chromosomal aberrations and their clinical significance in renal neoplasms. BioMed Res Int 2015;2015:476508. https://doi.org/10.1155/2015/476508.
[31] Monzon FA, Alvarez K, Peterson L, Truong L, Amato RJ, Hernandez-McClain J, et al. Chromosome 14q loss defines a molecular subtype of clear-cell renal cell carcinoma associated with poor prognosis. Mod Pathol 2011;24:1470–9.
[32] Wang KL, Weinrach DM, Luan C, Han M, Lin F, Teh BT, et al. Renal papillary adenoma–A putative precursor of papillary renal cell carcinoma. Hum Pathol 2007;38:239–46.
[33] Brunelli M, Eble JN, Zhang S, Martignoni G, Cheng L. Gains of chromosomes 7, 17, 12, 16, and 20 and loss of Y occur early in the evolution of papillary renal cell neoplasia: a fluorescent in situ hybridization study. Mod Pathol 2003;16:1053–9.